A Study of the Reduction of Noise in IUE Spectra Obtained by Adding Extracted Spectra

1. INTRODUCTION

The analysis of IUE spectra is ultimately limited by the inherent resolution and noise of each spectrum. The resolution is a fixed parameter of the instrument but the noise can be affected by the operation of the system.

For this satellite it is not possible to reduce the noise simply by increasing the exposure times because the camera target becomes saturated. However, it is possible to trail a star across the large aperture thus increasing the effective target area and hence the effective exposure time. This technique is used for low resolution spectra (Heck 1981) but cannot be used for high resolution spectra.

Another option is to add spectra taken at different times. This can be used for low and high resolution spectra and is the subject of this paper. The results indicate the value of adding spectra currently available (e.g. in the World Data Centre) and also provide a basis for deciding whether further observations of a target would be of use.

Certain objects have already been extensively observed with IUE. The two such objects that were used here were HD120315 (Eta Uma) for which we had 16 LWR and 9 SWP spectra and HD219188 for which we had 8 SWP spectra. The spectra used were all high resolution, observed in either the small or large aperture (mostly small): Of the 33 spectra used in this study half were observed in the high radiation shift. The observations of Eta Uma were too short to be seriously affected, but one observation of HD 219188 was noticeably noisier because of this.

2. METHOD

2.1 Adding the spectra

The position of a few of the stronger interstellar lines were located on each image and were used to determine a veloicty shift with respect to a baseline image. The velocity shifts were then used to correct all the spectra in each group to the baseline image. This process of alignment was necessary to prevent degradation of the line profiles. For Eta Uma, the situation proved difficult because the interstellar lines were weak and the quality of the alignment was uncertain. Thus

* Reprinted from IUE ESA Newsletter No. 12, December, 1981

HD 219188, which has some strong interstellar lines, was also used to illustrate the retention of good resolution and the enhanced detection of weak features.

After they had been aligned, the spectra were rebinned to a common wavelength grid using linear interpolation and a sampling rate which was at least as great as that used in the original spectra. The spectral orders of interest were then summed using weighting factors which were proportional to the mean flux in the order. Features such as reseaux and charged particle spikes were removed prior to the summation.

2.2 Measurement of noise in the spectrum

Six portions of each of the LWR and SWP spectra were selected for study. These were widely distributed over the camera target region and included regions about interstellar features of interest. An interactive program was used to fit, by least-squares, these regions using Chebyshev polynomials of order 4 or less. The percentage RMS deviations plotted in Figures 2, 3, and 4 were then calculated using the equation:

$$\% \text{ RMS DEVIATION} = \frac{100}{N}\sqrt{\sum_{i=1}^{N}\frac{(FN_i - FIT_i)^2}{FIT_i^2}}$$

where FN_i = fitted flux at point i

FIT_i = fitted flux at point i

N = number of points

An empirical value for the ratio of signal to noise may be obtained by dividing 100 by the percentage RMS Deviation.

This program was applied to single spectra and then to summed spectra. Where possible the summed spectra included different samples of the single spectra to indicate the spread of values.

3. RESULTS

Figure 1 shows the polynomial fitted to the continuum about the Mg II λ2802 Å interstellar line. The fits were well behaved for all of the measurements, requiring 2nd order polynomials for continuum regions and 3rd or 4th order polynomials for regions where the interstellar line was embedded in a

stellar profile (e.g., ZnII and MgI in Figure 5). Figures 1 and 5 also show the significant reduction in the noise levels which result from adding 5 or more spectra.

Figures 2 and 3 show the reduction in percentage RMS deviation with increasing numbers of summed spectra. The similarities between the curves are striking, showing that the general behaviour is independent of the position on the camera target. For most of the examples, the percentage RMS deviation approaches a constant value, about 3, corresponding to an empirical signal to noise ratio of 33. The greater part of the improvement, for these images, has been attained after summing five spectra. This is illustrated in Figures 2e and f where the summing of up to sixteen spectra caused no further improvement.

However, two exceptions (Figures 2a and 3f), which correspond to the regions to the regions having the lowest mean flux levels, show poorer behaviour. The percentage RMS deviations are 5 and 8 respectively after summing eight spectra Figure 4 illustrates the dependence on the mean flux level in the extracted spectrum. The spectra in this study were extracted using the STAK and TRAK procedure developed in the UK (Giddings and Settle 1980), this has similar resolution but a higher sampling rate than the old IUESIPS. However for this figure the extracted FN's have been scaled to be the same as those for the old IUESIPS. Since the behaviour of the SWP and LWR camera is so similar in this study, the two sets of data were plotted together and follow the same curve within the uncertainties of the measurements. Clearly, for extracted fluxes above 10000 FN (LWR) and 6000 FN (SWP), one generally needs only to sum about five spectra after which the noise in the spectrum is dominated by the noise in the extraction process. Below this level more spectra are required, as is illustrated both by the poorer percentage RMS deviation and the greater difference between the values obtained for the sum of five spectra and the sum of eight spectra. The general levels of noise for single spectra are also shown.

Figure 5 illustrates further advantages of adding spectra: the interstellar lines of MgII ($\lambda\lambda$1239, 1240 Å), which are lost in the noise of any single spectrum of HD219188, stand

out clearly in the sum of eight spectra; the ZnII λ2026.2 Å MgI λ2026.5 Å blend is not degraded by the addition of eight spectra, whereas the continuum has, as in many other regions, become more clearly defined. Images taken in the large and small apertures have their reseaux in different places, as do also some images taken at well separated time intervals, or in different parts of the large aperture. On adding the spectra it is possible to have sufficient overlap for the reseaux to be absent in the summed spectrum.

4. CONCLUSIONS

For spectra where the regions of interest have extracted fluxes of more than 10000 FN (LWR) or 6000 FN (SWP), the summing of more than five spectra is probably unwarranted. Adding spectra in the manner described in Section 2, causes no degradation of the line profiles provided the velocity correction is applied before adding. The shape of stellar lines within which interstellar lines are sometimes embedded can be more clearly identified. For this work the spectra were weighted with the mean net flux before adding; a possible improvement would be to weight the spectra using the percentage RMS deviation.

Kym West
Tom Shuttleworth
Dpt. of Physics & Astronomy
University College London

REFERENCES

Giddings, J., and Settle, J., 1980, SRC IUE Newsletter, 5, 11. (see also Gidding, J., this Newsletter page 22)
Heck, A., 1981, ESA IUE Newsletter, 9, 10.

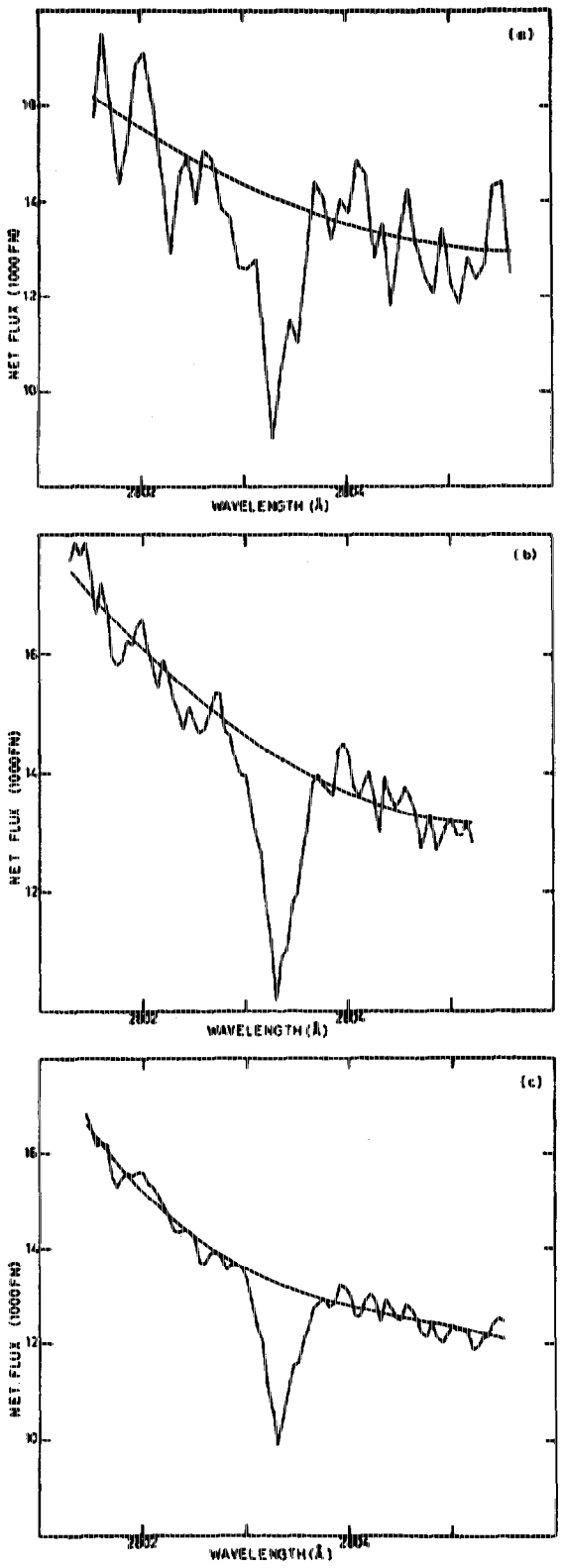

FIGURE 1 - Fit to the continuum about the MgII 2802.7 interstellar line in the spectrum of Eta Uma, A) for an individual image, b) after summing 5 spectra, c) after summing 9 spectra.

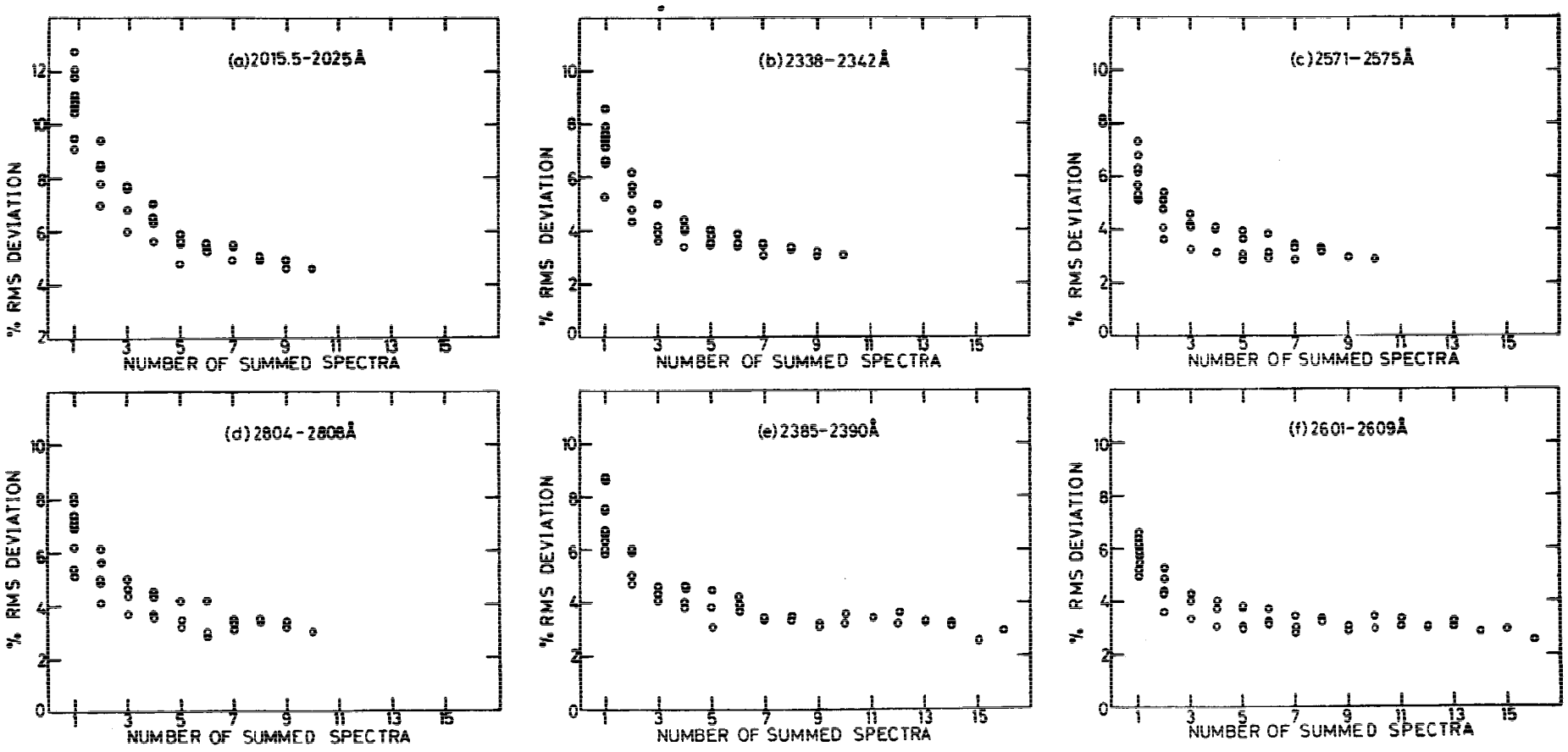

FIGURE 2 - Graphs showing the reduction in % RMS deviation about polynomial fits to the spectra of Eta Uma for six regions of the long wavelength high resolution images.

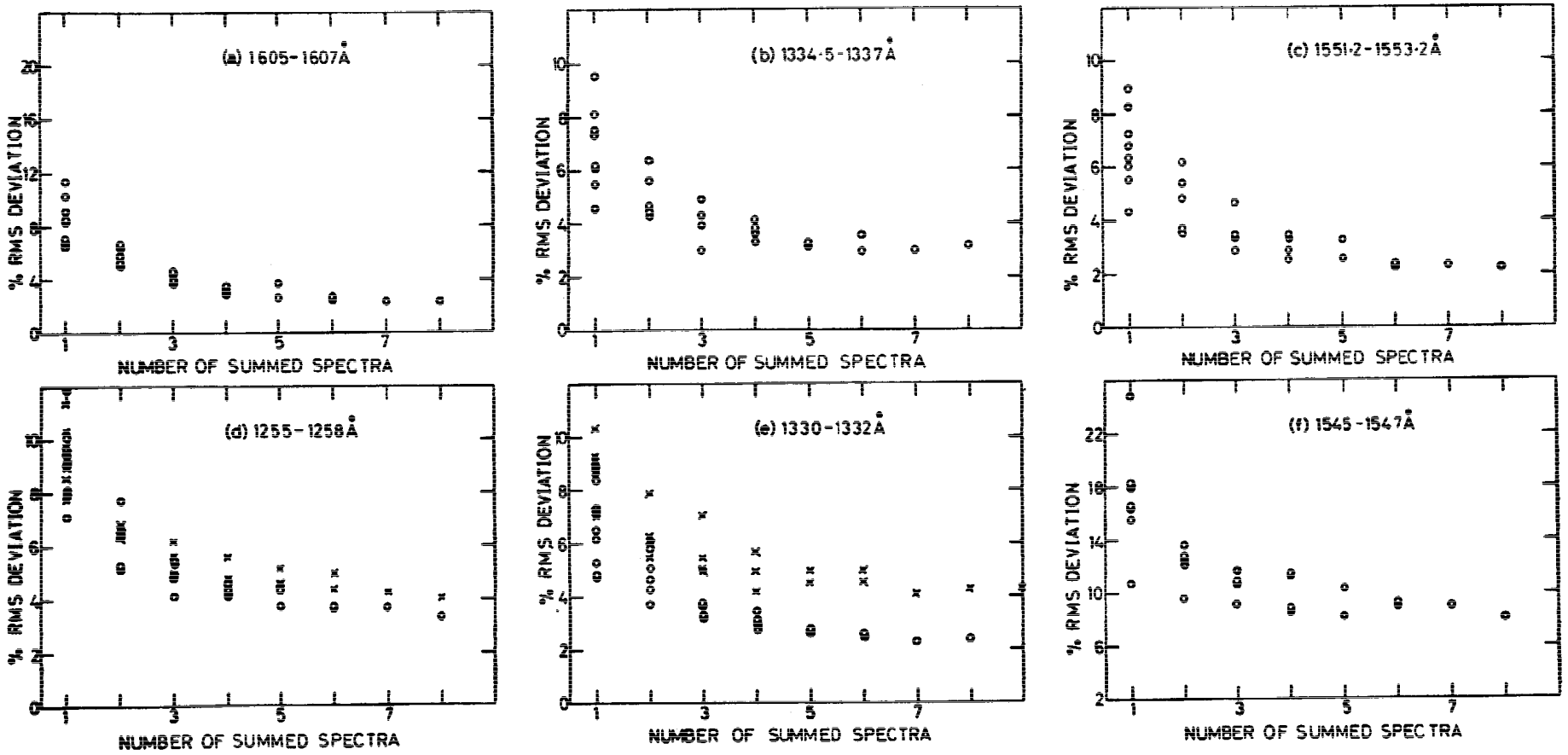

FIGURE 3 - Graphs showing the reduction in % RMS deviation about polynomial fits to the spectra of HD 219288 (o) and Eta Uma for six regions of the short wavelength high resolution images.

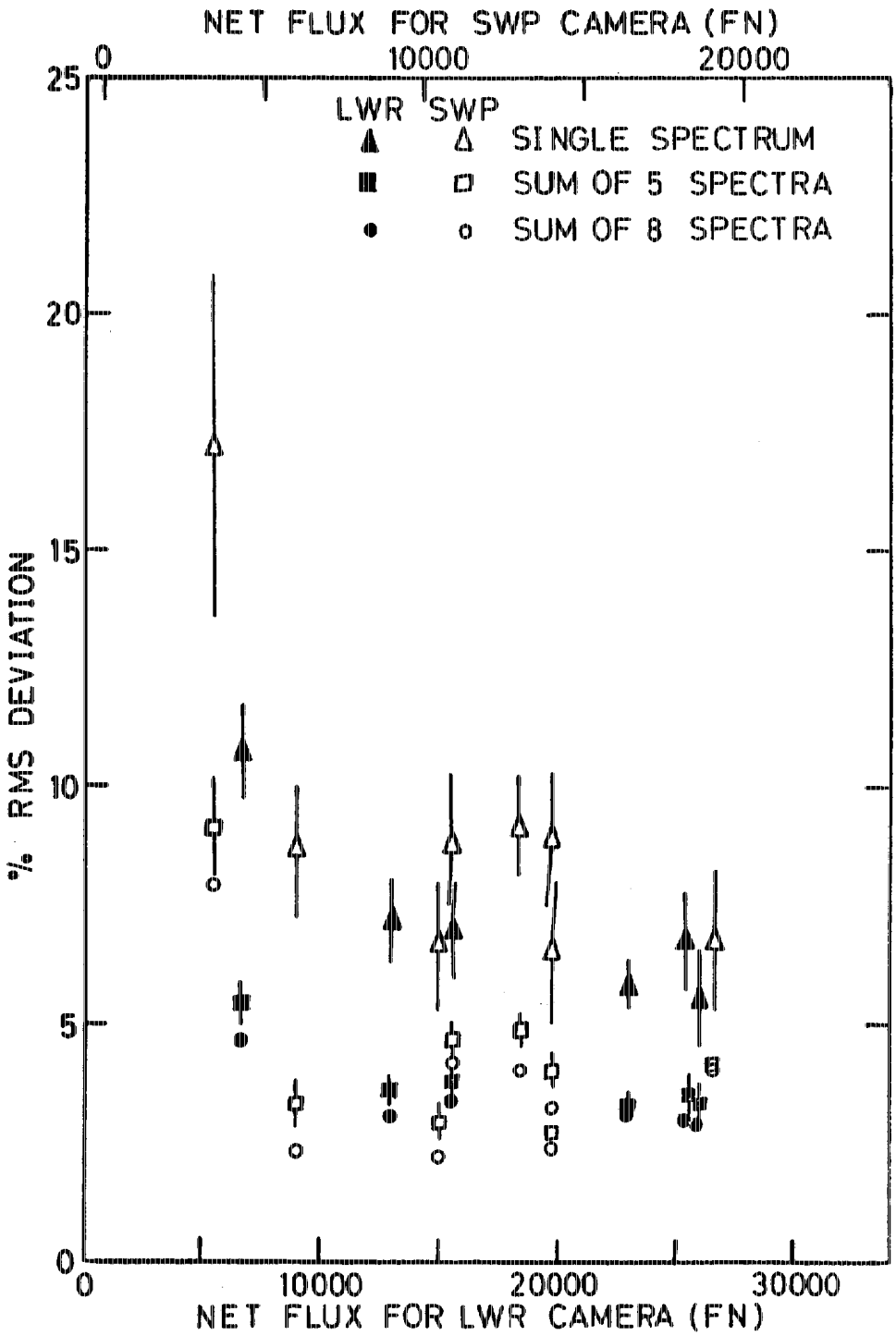

FIGURE 4 - The % RMS deviation for single and summed spectra plotted against the mean FN of each of the spectral regions used in Figures 2 and 3. The SWP axis has been rescaled to allow for the differing maximum FN values used in the photometric correction. The offset zero results from the omission of the background in the rescaling, although the 2000 FN correction was included.

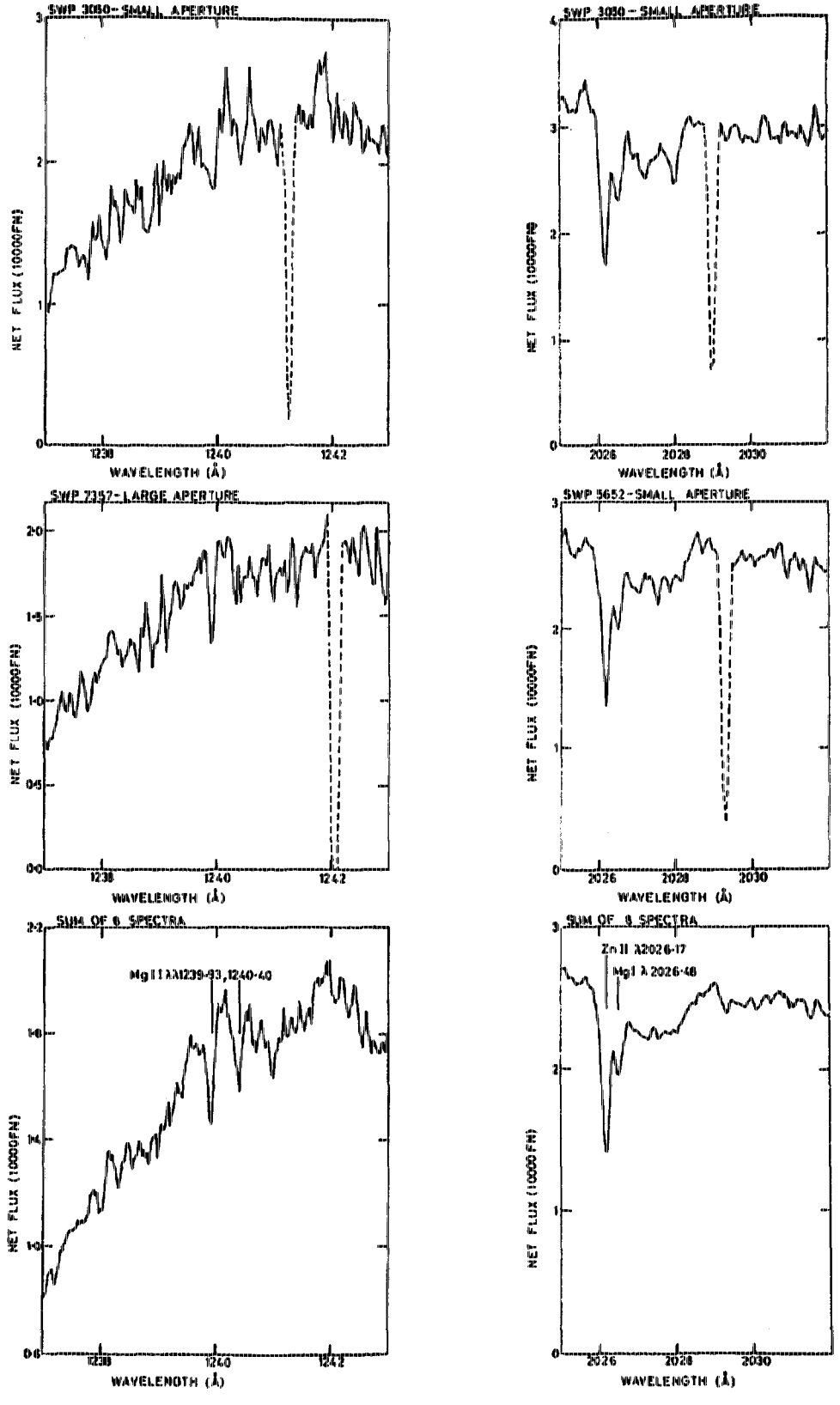

FIGURE 5 - Sample portions of the spectrum of HD 219188 from single spectra (top two rows) and from the sum of 8 spectra. The reduction in noise is evident as is the detection of MgII in the summed spectrum. The removal of a reseau and the clarification of the stellar profile in the summed spectrum are also shown.